Analysis of Head Loss in Pipe System Components:
Quasi-one-Dimensional Nozzle Flow

Charles Ndambuki Muli

School of Education, The Presbyterian University of East Africa, P.O. Box 387-00902, Kikuyu, Kenya.
mcndambuki@gmail.com

Abstract

The problem under investigation is to determine the flow-field variables that is the total head which is the sum total of Elevation head, velocity head   and pressure head instantaneous distributions as a function of distance through the nozzle up to "steady-state" solution that is, when the result approach the stage where the flow-field variables are not materially changing any more. The finite difference method is used to arrive at the results. Effects of temperature and density on velocity and pressure are analyzed with the help of a graph and table. It is found that the total head loss needed to accelerate the fluid through the constriction/the nozzle throat causes fluid velocity to increase.

Keywords: Quasi-one-dimensional flow, Head loss, Incompressible flow, Steady state flow.

Nomenclature

Symbol	Quantity
a	Acceleration of fluid element
A	The extend of a region (Area)
C_c	Coefficient of contraction
cv	Control volume
D	Diameter of pipe
F	Resultant forces acting on fluid mass
F_s	Surface forces
g	Acceleration due to gravity
i, j, k	Unit vectors along the $x, y,$ and z-axes
K	Loss coefficient
l	Length of the pipe (model)
m	Mass of the fluid element
n	Unit vector along normal to a streamline
P	Fluid Pressure
Q	Rate of mass flow
Re	Reynolds's number
u, v, w	Components of velocity along x, y, z respectively
v	Mean velocity of flow

Greek Symbols

V	Kinetic viscosity of fluid
∇	Laplace operator
Σ	Summation
σ	Normal stress
τ	Shearing stress
θ	Angle subtended by the curved part
γ	Normal force due to weight
α	Angle of convergence
ρ	Density

1. Introduction

Although the area of the nozzle changes as a function of distance along the nozzle, $x,$ and therefore in reality the flow field is two-dimensional (the flow varies in the two-dimensional xy space), we make the assumption that the flow properties vary only with x; this is tantamount to assuming uniform flow properties across any given cross section. Such flow is defined as *quasi-one-dimensional* flow

Pipe system components are encountered in many engineering and domestic applications, so fitting them up in a certain way that ensures all forces resulting may be balanced and hence absorbed within the supporting

structures without damage to them, that is, structure like for example a wall. Although, in practice turbulent flow conditions prevail in majority of engineering applications, differential-analytical studies of laminar flow in pipe are restricted to low Reynolds's number. A classically investigated problem in dynamics of a fluid is that in the circular straight pipe lying in any orientation that is Poiseuille-Hagen problem Gaerde (1990)

Simplifications of geometry and boundary condition by employing suitable assumption are usually considered in any model, however, in experiments and applications next to laminar flow, (with low Reynolds's numbers) velocity changes causes considerable forces on the parts of the pipe Beek (1985)who gives a method of procedure for calculating the magnitude and direction of this force.

Analysis of this simplified problem provides sound basis for comparison of analytical methods for example, finite difference method and the differential methods, and the possibility of gaining physical insight into related problems of practical importance. Both analytic and experimental studies have been carried out in particular for laminar and steady-state flow. A wide range of analytical investigation of this type of problem has been presented with different model of studies by authors such as Douglas *et al*. (1995) and comparison research on the problem was presented by Triton (1985)

A review of the literature on confined flow in various geometrics with different types of boundary conditions as well as a section on analysis was presented by Beek (1985). A comprehensive review concerning laminar flow in enclosed channels had earlier been presented by Roy and Daugherty, (1986)

In past, differential calculus studies were restricted to laminar flow, due to the difficulties on analysis and interpretation of the complex functions such as Navier-Stokes equations that define the general condition of flow motion by Munson *et al.* (1998) and the suitable boundary conditions that simplifies the situation. Consequently, a number of authors have attempted to model a number of these inviscid flows and the assumption of smooth channel sides.

There are many authors in this category like Manohar (1982), Douglas et *al.* (1995). This type of model simplifications resulted in better understanding and capability to transferring the knowledge gained into any shape of geometry of the problem under consideration.

Properties of flow at the pipe system components have been carried out extensively by Munson *et al*. (1998) and O'Neil *et al.* (1986) have adopted the streamline co-ordinate system in analysis of flow at this part of pipe system components to investigate variation of pressure and velocity distributions

In other areas of fluid analysis such as application of the theory of work-energy relationship, some writes especially in the field of physical sciences have considered fluid flow as stream of particles that can be considered for analysis independently and hence generalizing for the entire flow Gaerde (1990). Though this assumption of using particle theory on flow analysis has some weakness that is going to be highlighted later, it has been justified by Munson *et al*. (1998), by stating that;

"*Fluid flow can be treated approximately as particle flow. The work done on a particle by all forces acting on it is equal to the change in the kinetic energy of the particle which is basically Bernoulli's equation*"

Improvements in analytical techniques based on sound initial condition, extension to three dimensional calculations, additional work on laminar flow in various types of channels, for example cracks, analysis of pipe boundary functions as well as experimental validation of these techniques is considered as a landmark in analysis of flow of this type. The previous studies used the finite difference technique to exact solutions of fluid properties for example force. This method of finite difference technique and differential analysis gives accurate and reliable results and hence we have adopted them in our analysis.

In process of fluid passing through a pipe, the necessary conditions for pressure are to be provided to support the motion of fluid hence in our study there is an analysis of pressure at all sections required to support the desired flow. In addition pressure across each section will be obtained.

2.0 Formulation of the problem

We consider the steady, compressible, isentropic flow through a convergent-divergent nozzle as sketched in Fig.2.1. The flow at the inlet to the nozzle comes from a reservoir where the pressure and temperature are denoted by p_o, and T_o, respectively. The cross-sectional are of the reservoir is large (theoretically,$A \to \infty$), and hence velocity is very small$(V \to 0)$. Thus, p_o and T_o are the stagnation values, or *total* pressure and *total* temperature, respectively. The flow expands isentropic ally to supersonic speeds at the nozzle exit, where the exit pressure, temperature, velocity, and Mach number are denoted by p_e, T_e, V_e and M_e, respectively. The flow is locally subsonic in the convergent section of the nozzle, sonic at the throat (minimum area), and supersonic at the divergent section. The sonic flow $(M = 1)$ at the throat means that the local velocity at this location is equal to the local speed of sound. Using an asterisk to denote sonic flow values, we have at the throat$V = V^* = a^*$. Similarly, the sonic flow values of pressure and temperature are denoted by p^* and T^*, respectively. The area of the sonic

throat is denoted by A^*. We assume that at the given section, where the cross-sectional area is A, the flow properties are uniform across the section. Hence, although the area of the nozzle changes as a function of distance along the nozzle, x, and therefore in reality the flow field is two-dimensional (the flow varies in the two-dimensional xy space), we make the assumption that the flow properties vary only with x; this is tantamount to assuming uniform flow properties across any given cross section. Such flow is defined as *quasi-one-dimensional* flow.
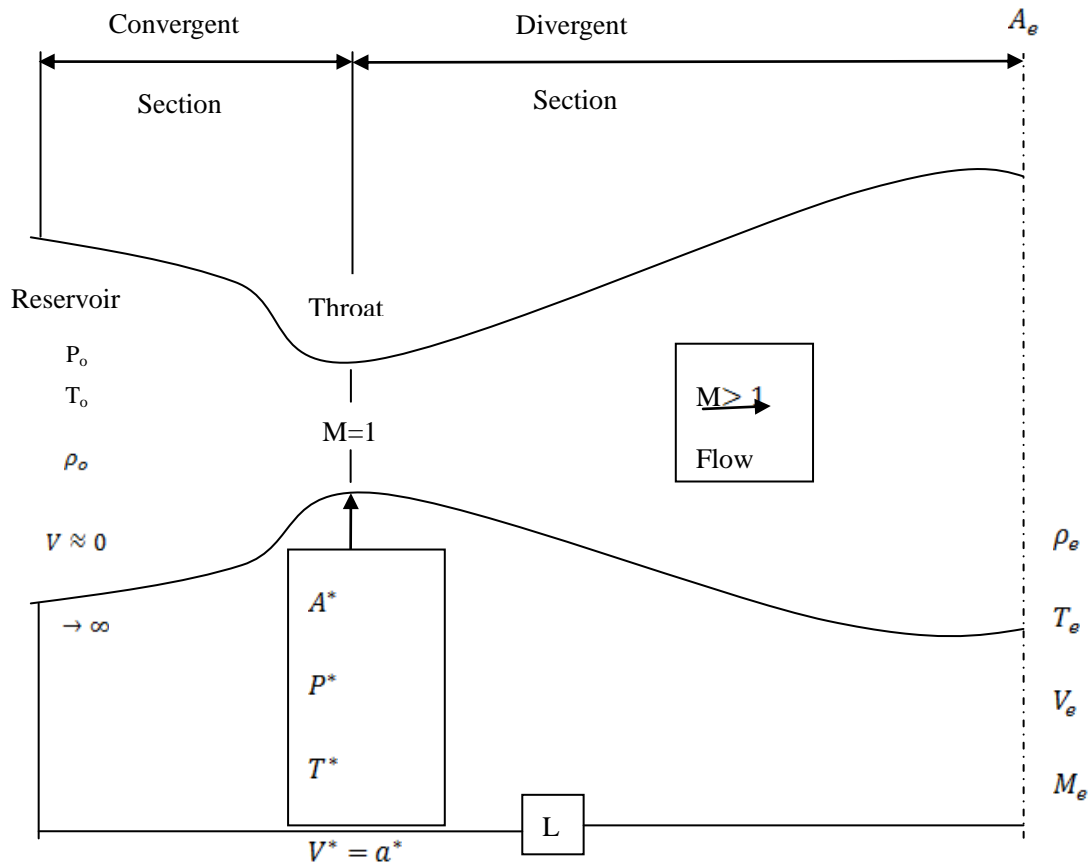

Figure 2.1: The geometry of the problem and the flow configuration with the coordinate system.

The governing continuity, momentum and energy equations for this quasi one-dimensional, steady, isentropic flow can be expressed, respectively, as

Continuity: $\rho_1 V_1 A_1 = \rho_2 V_2 A_2$ (2.1)

Momentum: $\rho_1 A_1 + \rho_1 V_1^2 A_1 + \int_{A_1}^{A_2} p\, dA = \rho_2 A_2 + \rho_2 V_2^2 A_2$ (2.2)

Energy: $h_1 + \frac{V_1^2}{2} = h_2 + \frac{V_2^2}{2}$ (2.3)

Where subscripts 1 & 2 denote different locations along the nozzle.

In addition, we have the perfect gas equation of state,

$p = \rho RT$ (2.4)

As well as the relation for a calorically perfect gas,

$$h = C_p T \tag{2.5}$$

Equation (2.1) to (2.5) can be solved analytically for the flow through the nozzle. Some results are as follows. The Mach number variation through the nozzle is governed exclusively by the area ratio A/A^*
Through the relation

$$\left(\frac{A}{A^*}\right)^2 = \frac{1}{M^2}\left[\frac{2}{\gamma+1}\left(1+\frac{\gamma-1}{2}M^2\right)\right]^{(\gamma+1)/(\gamma-1)} \tag{2.6}$$

where γ = ratio of specific heats C_p/C_v. For air at standard conditions, $\gamma = 1.4$. for a nozzle where A is specific as a function of x, the Eq.(2.6) allows the (implicit) calculation of M as a function of x. the variation of pressure, density and temperature as a function of Mach number (and hence as a function of A/A^*,thus x) is given respectively by

$$\frac{P}{P_o} = \left(1+\frac{\gamma-1}{2}M^2\right)^{-\gamma/(\gamma-1)} \tag{2.7}$$

$$\frac{\rho}{\rho_o} = \left(1+\frac{\gamma-1}{2}M^2\right)^{-\gamma/(\gamma-1)} \tag{2.8}$$

$$\frac{T}{T_o} = \left(1+\frac{\gamma-1}{2}M^2\right)^{-1} \tag{2.9}$$

The governing equations for unsteady, quasi-one dimensional flows are:
Continuity equation

$$\frac{\partial(\rho A)}{\partial t} + \frac{\partial(\rho A V)}{\partial x} = 0 \tag{2.10}$$

Momentum equation

$$\rho\frac{\partial V}{\partial t} + \rho V\frac{\partial V}{\partial x} = -\frac{\partial p}{\partial x} \tag{2.11}$$

Energy equation

$$\rho\frac{\partial e}{\partial t} + \rho V\frac{\partial e}{\partial x} = -p\frac{\partial V}{\partial x} - pV\frac{\partial(lnA)}{\partial x} \tag{2.12}$$

The reason for obtaining the energy equation in the form of Eq. (2.12) is that, for a calorically perfect gas, it leads directly to a form of the energy equation in terms of temperature T. for our solution of the quasi-one-dimensional nozzle flow of a calorically perfect gas, this is fundamental variable, and therefore it is convenient to deal with it as the primary dependent variable in the energy equation.
For a calorically perfect gas

$$e = C_V T$$

Hence

$$\rho C_V\frac{\partial T}{\partial t} + \rho V C_V\frac{\partial T}{\partial x} = -p\frac{\partial V}{\partial x} - pV\frac{\partial(lnA)}{\partial x} \tag{2.13}$$

The pressure can be eliminated from these equations by using the equation of state

$$p = \rho RT \tag{2.14}$$

Along with its derivative

$$\frac{\partial p}{\partial x} = R\left(\rho \frac{\partial T}{\partial x} + T \frac{\partial \rho}{\partial x}\right) \tag{2.15}$$

With this, we expand Eq. (2.10) and rewrite Eqs.(2.11) and (2.13), respectively, as

$$Continuity: \frac{\partial(\rho A)}{\partial t} + \rho A \frac{\partial V}{\partial x} + \rho V \frac{\partial A}{\partial x} + VA \frac{\partial \rho}{\partial x} = 0 \tag{2.16}$$

$$Momentum: \rho \frac{\partial V}{\partial t} + \rho V \frac{\partial V}{\partial x} = -R\left(\rho \frac{\partial T}{\partial x} + T \frac{\partial \rho}{\partial x}\right) \tag{2.17}$$

$$Energy: \rho C_V \frac{\partial T}{\partial t} + \rho V C_V \frac{\partial T}{\partial x} = -\rho RT\left[\frac{\partial V}{\partial x} - V \frac{\partial(\ln A)}{\partial x}\right] \tag{2.18}$$

2.1 The Finite difference technique

Here, we are interested in replacing a partial derivative with a suitable algebraic difference quotient, i.e., a *finite difference*. Most common finite difference representations of derivatives are based on Taylor's series expansions. For example, if $u_{i,j}$ denotes the x component of velocity at point (i,j), then the velocity $u_{i+1,j}$ at point $(i + 1, j)$ can be expressed in terms of a Taylor series expanded about point (i,j),   as follows

$$u_{i+1,j} = u_{i,j} + \left(\frac{\partial u}{\partial x}\right)_{i,j} \Delta x + \left(\frac{\partial^2 u}{\partial x^2}\right)_{i,j} \frac{(\Delta x)^2}{2} + \left(\frac{\partial^3 u}{\partial x^3}\right)_{i,j} \frac{(\Delta x)^3}{6} + \dots \tag{2.19}$$

Equation (2.14) is mathematically an exact expression for $u_{i+1,j}$ if (1) the number of terms is infinite and the series converges and /or (2) $\Delta x \to 0$.

From there we pursue the finite –difference representations of derivatives. Solving Eq. (2.14) for $(\partial u/\partial x)_{i,j}$, we obtain

$$\left(\frac{\partial u}{\partial x}\right)_{i,j} = \frac{(u_{i+1,j} - u_{i,j})}{\Delta x} - \left(\frac{\partial^2 u}{\partial x^2}\right)_{i,j} \frac{(\Delta x)^2}{2} - \left(\frac{\partial^3 u}{\partial x^3}\right)_{i,j} \frac{(\Delta x)^3}{6} + \dots \tag{2.20}$$

Finite-
difference
Representation

Truncation
error

In Eq. (2.20) the actual partial derivative evaluated at point (i,j) is given on the left side. The first term on the right side, namely $(u_{i+1,j} - u_{i,j})/\Delta x$, is a finite difference representation of the partial derivative. The remaining terms on the right side constitute the *truncation error*. That is, if we wish to *approximate* the partial derivative with the above algebraic finite-difference quotient,

$$\left(\frac{\partial u}{\partial x}\right)_{i,j} \approx \frac{(u_{i+1,j} - u_{i,j})}{\Delta x} \tag{2.21}$$

Then the truncation error in Eq. (2.20) tells us what is being neglected in this approximation. In Eq. (2.20), the lowest-order term in the truncation error involves Δx to the first power; hence, the finite-difference expression in Eq. (2.16) is called *first-order-accurate*. We can more formally write Eq. (2.20) as

$$\left(\frac{\partial u}{\partial x}\right)_{i,j} = \frac{(u_{i+1,j} - u_{i,j})}{\Delta x} + 0(\Delta x) \tag{2.22}$$

In Eq. (2.22), the symbol $0(\Delta x)$ is a formal mathematical notation which represents "terms of order Δx."

Equation (2.22) is a more precise notation than Eq. (2.21), which involves the "approximately equal" notation. Also referring to Fig.3.6, note that the finite-difference expression in Eq. (2.22) uses information to the *right* of the grid point (i,j); that is, it uses $u_{i+1,j}$ as well as $u_{i,j}$. No information to the left of (i,j) is used. As a result, the finite difference in Eq. (2.22) is called a *forward difference*. For this reason, we now identify the first-order-accurate difference representation for the derivative $(\partial u/\partial x)_{i,j}$ expressed by Eq. (2.22) as a *first-order-forward difference*, repeated below

$$\left(\frac{\partial u}{\partial x}\right)_{i,j} = \frac{(u_{i+1,j} - u_{i,j})}{\Delta x} + 0(\Delta x)$$

Let us now write a Taylor series expansion for $u_{i-1,j}$, expanded about $u_{i,j}$.

$$u_{i-1,j} = u_{i,j} + \left(\frac{\partial u}{\partial x}\right)_{i,j}(-\Delta x) + \left(\frac{\partial^2 u}{\partial x^2}\right)_{i,j}\frac{(-\Delta x)^2}{2} + \left(\frac{\partial^3 u}{\partial x^3}\right)_{i,j}\frac{(-\Delta x)^3}{6} + \dots$$

or

$$u_{i-1,j} = u_{i,j} - \left(\frac{\partial u}{\partial x}\right)_{i,j}\Delta x + \left(\frac{\partial^2 u}{\partial x^2}\right)_{i,j}\frac{(\Delta x)^2}{2} - \left(\frac{\partial^3 u}{\partial x^3}\right)_{i,j}\frac{(\Delta x)^3}{6} + \dots \tag{2.23}$$

Solving for $(\partial u/\partial x)_{i,j}$, we obtain

$$\left(\frac{\partial u}{\partial x}\right)_{i,j} = \frac{(u_{i,j} - u_{i-1,j})}{\Delta x} + 0(\Delta x) \tag{2.24}$$

The information used in forming the finite-difference quotient in Eq. (2.24) comes from the *left* of the grid point (i,j); that is, it uses $u_{i-1,j}$ as well as $u_{i,j}$. No information to the right of (i,j) is used. As a result, the finite difference in Eq. (2.19) is called a *rearward (or backward) difference*.
In this applications, first-order accuracy is sufficient.

2.2 The Mac Cormack's Method
The precise and appropriate technique (algorithm) for numerical solution by the finite-difference approach in this research work is Mac Cormack's method. This technique is an explicit finite- difference technique which is second-order-accurate in both space and time.For the purpose of illustration, let us address the solution of the Euler equations itemized (2.25) to (2.28) below

$$Continuity: \qquad \frac{\partial \rho}{\partial t} = -\left(\rho\frac{\partial u}{\partial x} + u\frac{\partial \rho}{\partial x} + \rho\frac{\partial v}{\partial y} + v\frac{\partial \rho}{\partial y}\right) \tag{2.25}$$

$$x\ momentum: \qquad \frac{\partial u}{\partial t} = -\left(u\frac{\partial u}{\partial x} + v\frac{\partial u}{\partial y} + \frac{1}{\rho}\frac{\partial p}{\partial x}\right) \tag{2.26}$$

$$y\ momentum: \qquad \frac{\partial v}{\partial t} = -\left(u\frac{\partial v}{\partial x} + v\frac{\partial v}{\partial y} + \frac{1}{\rho}\frac{\partial p}{\partial y}\right) \tag{2.27}$$

$$Energy: \qquad \frac{\partial e}{\partial t} = -\left(u\frac{\partial e}{\partial x} + v\frac{\partial e}{\partial y} + \frac{p}{\rho}\frac{\partial u}{\partial x} + \frac{p}{\rho}\frac{\partial v}{\partial y}\right) \tag{2.28}$$

Here we will address time-marching solution using Mac Cormack's technique. We will assume the flow field at each grid point is known at time t, and we proceed to calculate the flow field variables at the same grid points at time $t + \Delta t$ first, consider the density at the grid point (i,j) at time $t + \Delta t$. in Mac Cormack's method, this is obtained from

$$\rho_{i,j}^{t+\Delta t} = \rho_{i,j}^{t} + \left(\frac{\partial \rho}{\partial t}\right)_{av} \Delta t \qquad (2.29)$$

where $\left(\partial \rho / \partial t\right)_{av}$ is a representative mean value of $\partial \rho / \partial t$ between time t and $t + \Delta t$. In this method unlike the other methods, the value of $\left(\partial \rho / \partial t\right)_{av}$ in Eq. (2.29) is calculated so as to preserve second-order accuracy *without* the need to calculate values of the second time derivative $\left(\partial^2 \rho / \partial t^2\right)_{i,j}^{t}$, which is the term which involves a lot of algebra. With Mac Cormack's technique, this algebra is circumvented.

Similar relation are written for the other flow-field variables

$$u_{i,j}^{t+\Delta t} = u_{i,j}^{t} + \left(\frac{\partial u}{\partial t}\right)_{av} \Delta t \qquad (2.30)$$

$$v_{i,j}^{t+\Delta t} = v_{i,j}^{t} + \left(\frac{\partial v}{\partial t}\right)_{av} \Delta t \qquad (2.31)$$

$$e_{i,j}^{t+\Delta t} = e_{i,j}^{t} + \left(\frac{\partial e}{\partial t}\right)_{av} \Delta t \qquad (2.32)$$

Let us illustrate by using the calculation of density as an example. Return to Eq. (2.29). The average time derivative, $\left(\partial \rho / \partial t\right)_{av}$, is obtained from the predictor-corrector philosophy as follows.

Predictor step: In the continuity equation (2.25), replace the spatial on the right-hand side with *forward* differences.

$$\left(\frac{\partial \rho}{\partial t}\right)_{i,j}^{t} = -\left(\rho_{i,j}^{t} \frac{u_{i+1,j}^{t}-u_{i,j}^{t}}{\Delta x} + u_{i,j}^{t} \frac{\rho_{i+1,j}^{t}-\rho_{i,j}^{t}}{\Delta x} + \rho_{i,j}^{t} \frac{v_{i,j+1}^{t}-v_{i,j}^{t}}{\Delta y} + v \frac{\rho_{i,j+1}^{t}-\rho_{i,j}^{t}}{\Delta y}\right) \qquad (2.33)$$

In Eq. (2.33), all flow variables at time t are known values; i.e., the right-hand side is known. Now, obtain a *predicted* value of density, $(\bar{\rho})^{t+\Delta t}$, from the first two terms of a Taylor series, as follows

$$(\bar{\rho})_{i,j}^{t+\Delta t} = \rho_{i,j}^{t} + \left(\frac{\partial \rho}{\partial t}\right)_{i,j}^{t} \Delta t \qquad (2.34)$$

In Eq. (2.34), $\rho_{i,j}^{t}$ is known, and $\left(\partial \rho / \partial t\right)_{i,j}^{t}$ is known number from Eq. (2.33); hence $(\bar{\rho})_{i,j}^{t+\Delta t}$ is readily obtained. The value of $(\bar{\rho})_{i,j}^{t+\Delta t}$ is only a predicted value of the density; it is only first-order-accurate since Eq. (2.34) contains only the first-order terms in the Taylor series.

In a similar fashion, predicted values for u, v and e can be obtained, i.e,

$$(\bar{u})_{i,j}^{t+\Delta t} = u_{i,j}^{t} + \left(\frac{\partial u}{\partial t}\right)_{i,j}^{t} \Delta t \qquad (2.35)$$

$$(\bar{v})_{i,j}^{t+\Delta t} = v_{i,j}^{t} + \left(\frac{\partial v}{\partial t}\right)_{i,j}^{t} \Delta t \qquad (2.36)$$

$$(\bar{e})_{i,j}^{t+\Delta t} = e_{i,j}^{t} + \left(\frac{\partial e}{\partial t}\right)_{i,j}^{t} \Delta t \qquad (2.37)$$

In Eq. (2.34) to (2.37), numbers for the time derivatives on the right-hand side are obtained from Eqs. (2.26) to (2.28) respectively with forward differences used for the spatial derivatives, similar to those shown in Eq. (2.33) for the continuity equation.

Corrector step: In the corrector step, we first obtain a *predicted* value of the *time derivative* at time $t + \Delta t$, $(\partial \bar{\rho} / \partial t)_{i,j}^{t+\Delta t}$, by substituting the predicted values of $\rho, u,$ and v into the right side of the continuity equation, replacing the spatial derivatives with *rearward* differences.

$$\left(\frac{\overline{\partial\rho}}{\partial t}\right)_{i,j}^{t+\Delta t} =$$

$$\left[(\bar{\rho})_{i,j}^{t+\Delta t} \frac{(\bar{u})_{i,j}^{t+\Delta t}-(\bar{u})_{i-1,j}^{t+\Delta t}}{\Delta x} + (\bar{u})_{i,j}^{t+\Delta t} \frac{(\bar{\rho})_{i,j}^{t+\Delta t}-(\bar{\rho})_{i-1,j}^{t+\Delta t}}{\Delta x} + (\bar{\rho})_{i,j}^{t+\Delta t} \frac{(\bar{v})_{i,j}^{t+\Delta t}-(\bar{v})_{i-1,j}^{t+\Delta t}}{\Delta y} + (\bar{v})_{i,j}^{t+\Delta t} \frac{(\bar{\rho})_{i,j}^{t+\Delta t}-(\bar{\rho})_{i-1,j}^{t+\Delta t}}{\Delta y}\right]$$

(2.38)

The average value of the time derivative of density which appears in Eq. (2.30) is obtained from the arithmetic mean of $(\partial\rho/\partial t)_{i,j}^t$, obtained from Eq. (2.24), and $(\partial\bar{\rho}/\partial t)_{i,j}^{t+\Delta t}$, obtained from Eq. (2.38).

$$\left(\frac{\partial\rho}{\partial t}\right)_{av} = \frac{1}{2}\left[\left(\frac{\partial\rho}{\partial t}\right)_{i,j}^t + \left(\frac{\overline{\partial\rho}}{\partial t}\right)_{i,j}^{t+\Delta t}\right]$$

(2.39)

from Eq.   from Eq.
(2.33)   (2.38)

This allows us to obtain the final, "corrected" value of density at time $t+\Delta t$ from Eq.(2.29), repeated below:

$$\rho_{i,j}^{t+\Delta t} = \rho_{i,j}^t + \left(\frac{\partial\rho}{\partial t}\right)_{av}\Delta t$$

(2.40)

The predictor-corrector sequence described above yields the value of density at grid point (i,j) at the time $t+\Delta t$, as illustrated in Fig. 2.3 This sequence is repeated at all grid points to obtain the density throughout the flow field at time $t+\Delta t$. To calculate $u, v,$ and e at time $t+\Delta t$, the same technique is used, starting with Eqs. (2.30) to (2.32), and utilizing the momentum and energy equations in the form of Eqs. (2.26) to (2.28) to obtain the average time derivatives via the predictor-corrector sequence, using forward differences on the predictor and rearward differences on the corrector.

Mac Cormack's technique as described above, because a two-step predictor-corrector sequence is used with forward differences on the predictor and with rearward differences on the corrector, is a second-order-accurate method. Unlike other methods, Mac Cormack's method does *not* require the second order derivatives and therefore much easier to apply, because there is no need to evaluate the second order derivatives.

3. Methodology

3.1 Solution of the problem by Finite Difference expressions using Mac Cormack's Method

We now proceed to the next echelon, namely, the setting up of the finite-difference expressions using Mac-Cormack's explicit technique for the numerical solution of Eqs. (2.25), (2.26), and (2.28). To implement a finite-difference solution, we divide the x-axis along the nozzle into a number of discrete grid points. In Fig.2.1, the first grid point, labeled point 1, is assumed to be in the reservoir. The points are evenly distributed along the x axis, with Δx denoting the spacing between the grid points. The last point namely, that at the nozzle exit, is denoted by N; we have a total number of N grid points distributed along the axis. Point i is simply an arbitrary grid point, with points $i-1$ and $i+1$ as the adjacent points. Since the Mac-Cormack's technique is a predictor-corrector method and in the time marching approach, the flow-field variables at time t, we use the difference equations to solve explicitly for the variables at time $t+\Delta t$.

First, consider the predictor step. To reduce the complexity of the notation, we will drop the use of the prime to denote a dimensionless variable. In what follows, all variables are the non-dimensional variables, denoted earlier by the prime notation. Analogous to Eq. (2.17), from Eq. (2.20) we have

$$\left(\frac{\partial\rho}{\partial t}\right)_i^t = -\rho_i^t \frac{V_{i+1}^t-V_i^t}{\Delta x} - \rho_i^t V_i^t \frac{\ln A_{i+1}-\ln A_i}{\Delta x} - V_i^t \frac{\rho_{i+1}^t-\rho_i^t}{\Delta x}$$

(3.1)

From Eq.(2.26), we have

$$\left(\frac{\partial V}{\partial t}\right)_i^t = -V_i^t \frac{V_{i+1}^t-V_i^t}{\Delta x} - \frac{1}{\gamma}\left(\frac{T_{i+1}^t-T_i^t}{\Delta x} + \frac{T_i^t}{\rho_i^t}\frac{\rho_{i+1}^t-\rho_i^t}{\Delta x}\right)$$

(3.2)

From Eq. (2.28), we have

$$\left(\frac{\partial T}{\partial t}\right)_i^t = -V_i^t \frac{T_{i+1}^t - T_i^t}{\Delta x} - (\gamma - 1)T_i^t \left[\frac{V_{i+1}^t - V_i^t}{\Delta x} + V_i^t \frac{\ln A_{i+1} - \ln A_i}{\Delta x}\right] \tag{3.3}$$
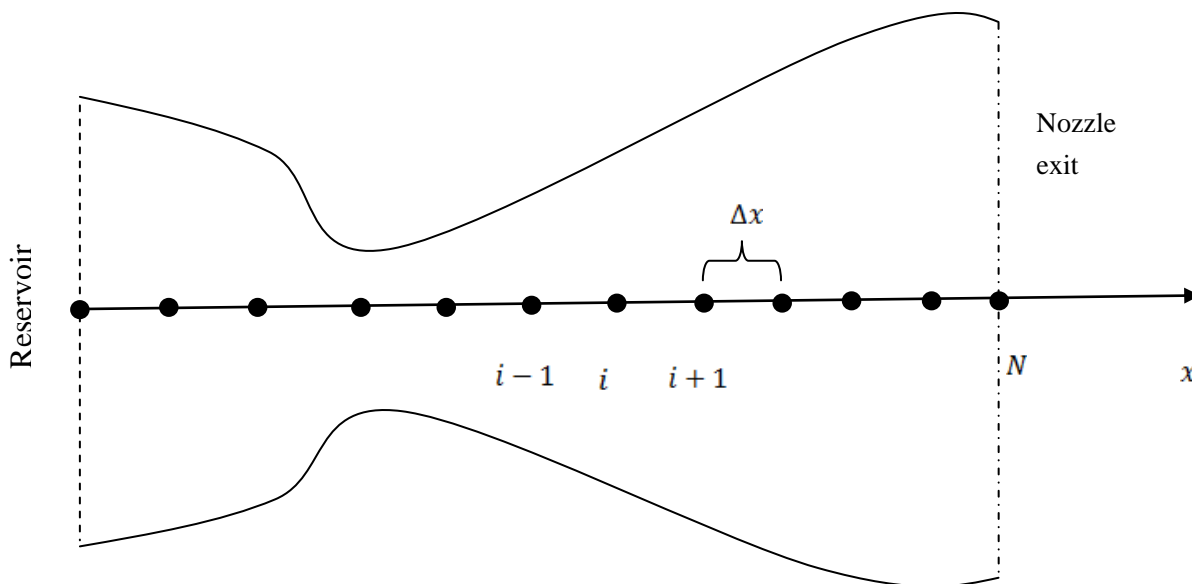

Figure 2: Grid point distribution along the nozzle

Analogous to Eqs.(2.40) to (2.43), we obtain predicted values of ρ, V and T, denoted by the barred quantities, from

$$\bar{\rho}_{i,j}^{t+\Delta t} = \rho_i^t + \left(\frac{\partial \rho}{\partial t}\right)_{i,j}^t \Delta t \tag{3.4}$$

$$\bar{V}_{i,j}^{t+\Delta t} = V_i^t + \left(\frac{\partial V}{\partial t}\right)_{i,j}^t \Delta t \tag{3.5}$$

$$\bar{T}_{i,j}^{t+\Delta t} = T_i^t + \left(\frac{\partial T}{\partial t}\right)_{i,j}^t \Delta t \tag{3.6}$$

In Eqs. (3.4) to (3.6) ρ_i^t, V_i^t, and T_i^t are known values at time t. Numbers for the time derivatives in Eqs. (3.4) to (3.6) are supplied directly by Eqs.(3.1) to (3.3).

Moving to the corrector step, we return to Eqs. (2.6), (2.8), and (3.0) and replace the spatial derivatives with rearward differences, using the predicted (barred) quantities. Analogous to Eq. (2.33) we have from Eq. (2.6),

$$\left(\frac{\overline{\partial \rho}}{\partial t}\right)_i^{t+\Delta t} = -\bar{\rho}_i^{t+\Delta t} \frac{\bar{V}_i^{t+\Delta t} - \bar{V}_{i-1}^{t+\Delta t}}{\Delta x} - \bar{\rho}_i^{t+\Delta t} \bar{V}_i^{t+\Delta t} \frac{\ln A_i - \ln A_{i-1}}{\Delta x} - \bar{V}_i^{t+\Delta t} \frac{\bar{\rho}_i^{t+\Delta t} - \bar{\rho}_{i-1}^{t+\Delta t}}{\Delta x} \tag{3.7}$$

From Eq. (2.8), we have

$$\left(\frac{\overline{\partial V}}{\partial t}\right)_i^{t+\Delta t} = -\bar{V}_i^{t+\Delta t} \frac{\bar{V}_i^{t+\Delta t} - \bar{V}_{i-1}^{t+\Delta t}}{\Delta x} - \frac{1}{\gamma}\left(\frac{\bar{T}_i^{t+\Delta t} - \bar{T}_{i-1}^{t+\Delta t}}{\Delta x} + \frac{\bar{T}_i^{t+\Delta t}}{\bar{\rho}_i^{t+\Delta t}} \frac{\bar{\rho}_i^{t+\Delta t} - \bar{\rho}_{i-1}^{t+\Delta t}}{\Delta x}\right) \tag{3.8}$$

From Eq. (3.0), we have

$$\left(\frac{\overline{\partial T}}{\partial t}\right)_i^{t+\Delta t} = -\bar{V}_i^{t+\Delta t}\frac{\bar{T}_i^{t+\Delta t}-\bar{T}_{i-1}^{t+\Delta t}}{\Delta x} - (\gamma-1)\bar{T}_i^{t+\Delta t}\left[\frac{\bar{V}_i^{t+\Delta t}-\bar{V}_{i-1}^{t+\Delta t}}{\Delta x} + \bar{V}_i^{t+\Delta t}\frac{lnA_i-lnA_{i-1}}{\Delta x}\right] \tag{3.9}$$

Analogous to Eq. (2.33), the average time derivatives are given by

$$\left(\frac{\partial\rho}{\partial t}\right)_{av} = \frac{1}{2}\left[\left(\frac{\partial\rho}{\partial t}\right)_i^t + \left(\frac{\overline{\partial\rho}}{\partial t}\right)_i^{t+\Delta t}\right] \tag{3.10}$$

$$\left(\frac{\partial V}{\partial t}\right)_{av} = \frac{1}{2}\left[\left(\frac{\partial V}{\partial t}\right)_i^t + \left(\frac{\overline{\partial V}}{\partial t}\right)_i^{t+\Delta t}\right] \tag{3.11}$$

$$\left(\frac{\partial T}{\partial t}\right)_{av} = \frac{1}{2}\left[\left(\frac{\partial T}{\partial t}\right)_i^t + \left(\frac{\overline{\partial T}}{\partial t}\right)_i^{t+\Delta t}\right] \tag{3.12}$$

Finally analogous to Eqs. (2.35) to (2.38), we have the corrected values of the flow-field variables at the time $t+\Delta t$

$$\rho_i^{t+\Delta t} = \rho_i^t + \left(\frac{\partial\rho}{\partial t}\right)_{av}\Delta t \tag{3.13}$$

$$V_i^{t+\Delta t} = V_i^t + \left(\frac{\partial V}{\partial t}\right)_{av}\Delta t \tag{3.14}$$

$$T_i^{t+\Delta t} = T_i^t + \left(\frac{\partial T}{\partial t}\right)_{av}\Delta t \tag{3.15}$$

3.1.1 Boundary Conditions

We note that grid points *1* and *N* represent the two boundary points on the x axis. Point *1* is essentially in the reservoir; it represents an *inflow* boundary, with flow coming from the reservoir and entering the nozzle. In contrast, point *N* is an *outflow* boundary, with flow leaving the nozzle at the exit.

Subsonic inflow boundary (point 1):   Here we must allow one variable to float; we choose the velocity V_1 , because on a physical basis we know the mass flow through the nozzle must be allowed to adjust to the proper steady state, allowing V_1 to float makes the most sense as part of this adjustment. The value of V_1 changes with time and is calculated from the information provided by the flow-field solution over the internal points. (The *internal* points are those not on a boundary, I.e., points 2 through $N-1$ in Fig.3.3). We use linear extrapolation from points 2 and 3 to calculate V_1. Here, the slope of the linear extrapolation line is determined from the points 2 and 3 as

$$Slope = \frac{V_3-V_2}{\Delta x}$$

Using this slope to find V_1 by linear extrapolation, we have

$$V_1 = V_2 - \frac{V_3-V_2}{\Delta x}\Delta x \quad \text{Or} \quad V_1 = 2V_2 - V_3 \tag{3.16}$$

All other flow-field variables are specified. Since point 1 is viewed as essentially the reservoir, we stipulate the density and temperature at the point 1 to be their respective stagnation values, ρ_o and T_o, respectively. These are

held *fixed*, independent of time.

Hence, in terms of the *non-dimensional* variables, we have

$$\left.\begin{array}{l}\rho_1 = 1 \\ T_1 = 1\end{array}\right\} \text{ Fixed, independent of time} \tag{3.17}$$

Supersonic outflow boundary (point N): Here, we must allow *all* flow-field variables to float. We again choose touse linear extrapolation based on the flow-field values at the internal points. Specifically, we have, for the *non-dimensional* variables

$$V_N = 2V_{N-1} - V_{N-2} \tag{3.18a}$$
$$\rho_N = 2\rho_{N-1} - \rho_{N-2} \tag{3.18b}$$
$$T_N = 2T_{N-1} - T_{N-2} \tag{3.18c}$$

3.1.2 Nozzle Shape and Initial Conditions

The nozzle shape, $A = A(x)$, is specified and held fixed, independent of time. For the case illustrated in this section, we choose a parabolic area distribution given by

$$A = 1 + 2.2(x - 1.5)^2 \qquad 0 \le x \le 3 \tag{3.19}$$

Note that $x = 1.5$ is the throat of the nozzle, that the convergent section occurs for $x < 1.5$, and that the divergent section occurs for $x > 1.5$. this nozzle shape is drawn to scale in Fig.2.

To start the time-marching calculations, we must stipulate *initial* conditions for $\rho, T,$ and V as a function of x; that is, we must set up values of $\rho, T,$ and V at time $t = 0.$ In theory, these initial conditions can be purely arbitrary. In practice, there are.

In the present problem, we know that ρ and T *decrease* and V *increase* as the flow expands through the nozzle. Hence, we choose initial conditions that *qualitatively* behave in the same fashion.

For simplicity, let us assume linear variations of the flow-field variables, as a function of x.

For the present case, we assume the following values at time $t = 0.$

$$\left.\begin{array}{l}\rho = 1 - 0.3146x \\ T = 1 - 0.2314x \\ V = (0.1 + 1.09x)T^{1/2}\end{array}\right\} \text{ Initial conditions at } t = 0 \tag{3.20a, 3.20b, 3.20c}$$

3.3.3 Numerical Results

The first step is to feed the nozzle shape and the initial conditions into the program. These are given by the Eq. (3.19) and (3.20); the resulting numbers are tabulated in the Table 1. The values of ρ, V and T given in this table are for $t = 0.$

Calculations associated with grid point i. We will choose $i = 16$, which is the grid point at the throat of the nozzle   from the initial data given in the Table 1

Defining a non-dimensional pressure as the local static pressure divided by the reservoir pressure p_o, the equation of state is given by

$$p = \rho T$$

Where $p, \rho,$ and T are *non-dimensional* values.   Thus, at grid point $i = 16$ we have

$$p_{16}^{t=\Delta t} = \rho_{16}^{t=\Delta t} T_{16}^{t=\Delta t} = 0.531(0.656) = 0.349$$

It remains to calculate the flow-field variables at the boundary points. At the subsonic inflow boundary

x	$\dfrac{A}{A^*}$	$\dfrac{\rho}{\rho_0}$	$\dfrac{V}{a_0}$	$\dfrac{T}{T_0}$
0	5.590	1.000	0.100	1.000
0.1	5.312	0.969	0.207	0.977
0.2	4.718	0.937	0.311	0.954
0.3	4.168	0.906	0.412	0.931
0.4	3.662	0.874	0.511	0.907
0.5	3.200	0.843	0.607	0.884
0.6	2.782	0.811	0.700	0.861
0.7	2.408	0.780	0.790	0.838
0.8	2.078	0.748	0.877	0.815
0.9	1.792	0.717	0.962	0.792
1.0	1.550	0.685	1.043	0.769
1.1	1.352	0.654	1.122	0.745
1.2	1.198	0.622	1.197	0.722
1.3	1.088	0.591	1.268	0.699
1.4	1.022	0.560	1.337	0.676
1.5	1.000	0.528	1.402	0.653
1.6	**1.022**	**0.497**	**1.463**	**0.630**
1.7	1.088	0.465	1.521	0.607
1.8	1.198	0.434	1.575	0.583
1.9	1.352	0.402	1.625	0.560
2.0	1.550	0.371	1.671	0.537
2.1	1.792	0.339	1.713	0.514
2.2	2.078	0.308	1.750	0.491
2.3	2.408	0.276	1.783	0.468
2.4	2.782	0.245	1.811	0.445
2.5	3.200	0.214	1.834	0.422
2.6	3.662	0.182	1.852	0.398
2.7	4.168	0.151	1.864	0.375
2.8	4.718	0.119	1.870	0.352
2.9	5.312	0.088	1.870	0.329
3.0	5.950	0.056	1.864	0.306

Table 1: Nozzle shape and initial conditions

$(i = 1)$, V_1 is calculated by linear extrapolation from grid points 2 and 3. At the end of the corrector step, from a calculation identical to that given above, the values of V_2 and V_3 at time $t = \Delta t$ are $V_2 = 0.212$ and $V_3 = 0.312$.

Thus, from Eq. (3.20), we have

$V_1 = 2V_2 - V_3 = 2(0.212) - 0.312 = 0.111$

At the supersonic outflow boundary $(i = 31)$ all the flow-field variables are calculated by linear extrapolation from Eqs. (3.24a) to (3.24c). at the end of the corrector step, from a calculation identical to that given above, $V_{29} = 1.884$, $V_{30} = 1.890$, $\rho_{29} = 0.125$, $\rho_{30} = 0.095$, $T_{29} = 0.354$, and $T_{30} = 0.332$. when these values are inserted into Eqs. (3.46a) to (3.46c), we have $V_{31} = 2V_{30} - V_{29} 895 = 2(1.890) - 1.884 = 1.895$

$\rho_{31} = 2\rho_{30} - \rho_{29} = 2(0.095) - 0.125 = 0.066$
$T_{31} = 2T_{30} - T_{29} = 2(0.332) - 0.354 = 0.309$

With this, we have completed the calculation of all the flow-field variables at all the grid points after the first time step, i.e., at $t = \Delta t$.

At this stage, the steady state (for all practical purposes) has been achieved and simply stops the calculation after a prescribed number of time steps. Look at the results, and see if they have approached the stage where the flow-field variables are not materially changing any more.

Comparing the flow-field results obtained (Table 2) after one step with the same quantities at the previous time,

we see that the flow-field variables have *changed*. For example, the non-dimensional density at the throat (where $A = 1$) has changed from 0.528 to 0.531, a 0.57 percent change over one time step. This is natural behavior of the time marching solution i.e., the flow-field variables change from one time step to the next. However, in the approach toward the steady-state solution, at larger values of time (after a large number of time steps), the *changes* in the flow-field variables from one time step   to the next becomes smaller and approach zero in the limit of large time.

I	$\frac{x}{L}$	$\frac{A}{A^*}$	$\frac{\rho}{\rho_0}$	$\frac{V}{a_0}$	$\frac{T}{T_0}$	$\frac{p}{p_0}$
1	0.000	5.950	1.000	0.111	1.000	1.000
2	0.100	5.312	0.955	0.212	0.972	0.928
3	0.200	4.718	0.927	0.312	0.950	0.881
4	0.300	4.168	0.900	0.411	0.929	0.836
5	0.400	3.662	0.872	0.508	0.908	0.791
6	0.500	3.200	0.844	0.603	0.886	0.748
7	0.600	2.782	0.817	0.695	0.865	0.706
8	0.700	2.408	0.789	0.784	0.843	0.665
9	0.800	2.078	0.760	0.870	0.822	0.625
10	0.900	1.792	0.731	0.954	0.800	0.585
11	1.000	1.550	0.701	1.035	0.778	0.545
12	1.100	1.352	0.670	1.113	0.755	0.506
13	1.200	1.198	0.637	1.188	0.731	0.466
14	1.300	1.088	0.603	1.260	0.707	0.426
15	1.400	1.022	0.567	1.328	0.682	0.387
16	1.500	1.000	0.531	1.394	0.656	0.349
17	1.600	1.022	0.494	1.455	0.631	0.312
18	1.700	1.088	0.459	1.514	0.605	0.278
19	1.800	1.198	0.425	1.568	0.581	0.247
20	1.900	1.352	0.392	1.619	0.556	0.218
21	2.000	1.550	0.361	1.666	0.533	0.192
22	2.100	1.792	0.330	1.709	0.510	0.168
23	2.200	2.078	0.301	1.748	0.487	0.146
24	2.300	2.408	0.271	1.782	0.465	0.126
25	2.400	2.782	0.242	1.813	0.443	0.107
26	2.500	3.200	0.213	1.838	0.421	0.090
27	2.600	3.662	0.184	1.858	0.398	0.073
28	2.700	4.168	0.154	1.874	0.376	0.058
29	2.800	4.718	0.125	1.884	0.354	0.044
30	2.900	5.312	0.095	1.890	0.332	0.032
31	3.000	5.950	0.066	1.895	0.309	0.020

Table 2.Flow-field variables after the first time step

4.0 Summary and Conclusions

The general conclusions we have made in this research study and also suggest areas for further research which have showed up during this research study.

4.1 Conclusions

In the foregoing sections we have showed that pressure for fully developed pipe flow is determined by a balance between the two forces:

     I. Temperature
     II. Density

a) From the graph plotted for the pressure and velocity across the nozzle length, it is clear that pressure decrease/head loss (needed to accelerate the fluid through the constriction/the nozzle throat at grid point $i = 15,$ where $A = 1$) causes fluid velocity to increase.
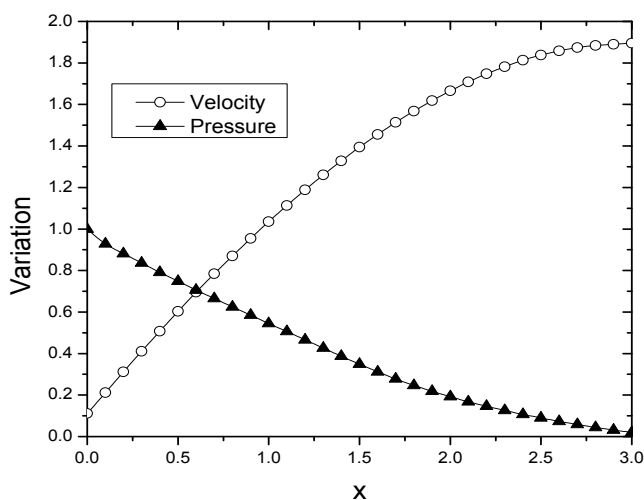
Figure 1: Variation of the velocity and pressure across the nozzle

The time-wise variations of the flow-field variables provided by Fig. 1, which shows the variation of v and p at the nozzle throat plotted versus the number of time steps.

b)   In analysis, the problem can be simplified by use of suitable symmetries of geometry. This mathematical problem can be simplified by taking suitable boundary conditions that are well considered and chosen before application.
c)   In this work, we demystified the mathematical jargon in the generalized mathematical formulae in textbooks by applying to the situation considered. Hence, we believe this can enhance understanding of such physical science as fluid mechanics and thus motivate many to appreciate, develop interest in studying it.

4.2 Recommendations for further study

In this project, we have assumed that the cross-section is uniform throughout, but any geometrical shape can be decided for inquest of varying the type of model to be either tapering or to contain orifices at any part of its entire length.

This can be done in some way such as:

(i.) The type of pipe may be tapering at the conical section of the model and let fluid enter from either ends.

(ii.) The model may be considered to have a feeder pipe to discharge into or drain the main pipe at any part of the entire length.

(iii.) Since the model assumes the pipe is flowing full, consideration should be done for partly full through an inclined or vertical pipe.

Acknowledgement

References

Beek, W.J (1985). *Transport phenomena*, John Wiley and Song Inc., UK.

Douglas, J.F. et al (1995). *Fluid Mechanics*, (3rd ed.). Long man Essex.

Gaerde, R.J. (1990). *Fluid Mechanics through problems*, Wiley Eastern Limited, Bombay.

Manohar, M. (1982). *Fluid Mechanics* **Vol**. One V. Kas   publishing house PVT LTD, New Delhi 1982.

Munson, B.R, et al (1998).   *Fundamentals of Fluid Mechanics*. (3rd ed.). John Wiley and sons Inc., New York.

O'neil, M, E, et al (1986). *Viscous and compressible fluid dynamics* ElhsHorwood, Chichester.

Roy, D, N. and Daugherty, R.L. (1986 & 1987).   *Applied fluid mechanics*, Affiliated East-west press PVT LTD, New Delhi.

Tritton, D.J. (1985).   *Physical fluid dynamics*, Van Nestrand Reinhold Co. Ltd, UK.